Phonon Density of States Measured by Inelastic Nuclear Resonant Scattering

W. Sturhahn, T. S. Toellner, and E. E. Alp
Advanced Photon Source, Argonne National Laboratory, Argonne, Illinois 60439

X. Zhang and M. Ando
Photon Factory, National Laboratory for High Energy Physics, Oho 1-1, Tsukuba, Ibaraki 305, Japan

Y. Yoda and S. Kikuta
Department of Applied Physics, Faculty of Engineering, The University of Tokyo, Hongo 7-3-1, Bunkyo-ku, Tokyo 113, Japan

M. Seto
Research Reactor Institute, Kyoto University, Sennan-gun, Osaka 590-04, Japan

C. W. Kimball and B. Dabrowski
Department of Physics, Northern Illinois University, De Kalb, Illinois 60115
(Received 16 December 1994)

The phonon density of states was measured by observing the nuclear resonant fluorescence of ^{57}Fe versus the energy of incident x rays from a synchrotron radiation beam. An energy resolution of 6 meV was achieved by use of high-resolution crystal optics for the incident beam. Extremely low background levels were obtained via time discrimination of the nuclear fluorescent radiation.

PACS numbers: 63.20.–e, 76.80.+y

Knowledge of the dynamics of atomic motion has been valuable in condensed matter physics [1]. It is possible to obtain this information by measurement of the phonon dispersion relation with slow neutrons or monochromatic light, the latter with a very restricted range in momentum transfer, along different directions of a single crystalline sample [2,3]. The data can be used to reconstruct the complete four-dimensional dispersion surface once a specific model for the interatomic forces has been chosen. The phonon density of states (DOS) is then calculated from the reconstructed dispersion relation [4]. In many cases of interest, single-crystal samples are not available or it might be sufficient to know the phonon DOS and not the complete dispersion relation. This situation can be accommodated by collecting the scattered neutrons over a large solid angle for those elements with an appreciable cross section for inelastic neutron scattering. The energy of the scattered neutrons has to be determined, e.g., by time-of-flight analysis, and the selected neutrons have to be discriminated against electronic scattering contributions and detector noise. The scattering of x rays was considered as an alternative method to analyze excitations in solids [5]. The x rays interact predominantly with the electrons in the solids, and vibrational excitations are accompanied by low energy electronic excitations.

In the present Letter, we use a recently reported method [6] that permits derivation of the phonon DOS directly from the measured data. We observed the absorption of x rays from the 14.4136-keV nuclear resonance of ^{57}Fe and the subsequent deexcitation by emission of K-fluorescence radiation. Nuclear resonances that are low in energy usually have a very narrow energy width, 4.66 neV for ^{57}Fe. Considering inelastic scattering, we may benefit from such a well-defined energy reference in the lattice. This allows tuning the energy of the incident x rays with respect to this resonance and not with respect to the energy of the scattered particle, which then would have to be determined. Furthermore, the deexcitation of the nucleus by emission of a conversion electron followed by fluorescence radiation takes place on a time scale of the lifetime of the nuclear resonance, 141 ns for ^{57}Fe. If the nucleus is excited by pulsed synchrotron radiation, the discrimination of nuclear resonant absorption from the electronic contribution is very efficiently done by counting only delayed fluorescence photons. Tuning the energy of the incident synchrotron radiation with respect to the nuclear resonance while monitoring the total yield of the delayed fluorescence photons gives a direct measure of the phonon DOS.

Nuclear resonances with low transition energies on the order of 10 keV can be coherently excited by synchrotron radiation with very high efficiency [7–9]. Besides the precise determination of hyperfine interaction parameters, these experiments permit determination of the Lamb-Mössbauer factor [10,11]. The incoherent scattering from a nuclear resonance was observed [12,13], but the signal was too weak for further analysis. The probability of such a process can be calculated from a self-correlation function of the displacement of the nucleus. Similar self-correlation functions were discussed earlier with respect to neutron scattering [14] and with respect to effects on the line shape of the nuclear resonance in Mössbauer transmission experiments [15]. The quantitative analysis gives reasonable

 0031-9007/95/74(19)/3832(4)$06.00 © 1995 The American Physical Society

probability for the excitation of the nuclear resonance with synchrotron radiation when the energy is tuned away by an amount needed for creation or annihilation of phonons. The arrival of a very short (<100 ps) synchrotron-radiation flash triggers the emission process of an inelastically scattered photon or of a conversion electron and subsequent fluorescence radiation. In both cases the delay of this emission is on the order of the natural lifetime of the nuclear resonance. The discrimination of the delayed events, which then signal the creation or annihilation of phonons from all other scattering contributions, which are prompt in time, is achieved by conventional timing methods. The energy resolution in the phonon spectrum is determined by the energy bandwidth of the incident synchrotron radiation.

In the present experiment, the 14.4136-keV resonance of the Mössbauer isotope ^{57}Fe was employed because of its large resonance cross section, the tolerable electronic absorption in the materials used, and the convenient lifetime. However, the method can be applied for any nuclear resonance of nuclei in solids, liquids, or gases.

The experiments were performed at the undulator beamline NE#3 at the 6.5-GeV KEK-AR synchrotron radiation facility in Tsukuba, Japan [16]. A high-heat-load monochromator, which consists of two symmetric silicon (111) reflections in a nondispersive setting, and a high-resolution, nested monochromator, as described earlier [17], were employed to achieve the required energy resolution. The high-resolution monochromator uses asymmetric silicon (422) and symmetric silicon (10 6 4) reflections. The synchrotron radiation incident on the ^{57}Fe-containing sample had an energy bandwidth of 6 meV at 14.4136 keV. An avalanche photodiode (APD) with an active area of 2 cm^2 was used to detect the emitted fluorescence radiation [18]. The photon flux on the sample was monitored with an ion chamber for proper normalization of the data.

The time delay between the output pulses of the APD detector and the bunch arrival signal that was derived from the RF of the storage ring was measured. The nonresonantly scattered radiation that appears promptly with respect to the bunch arrival signal was eliminated by counting in a time window of 30 to 600 ns after the arrival of the synchrotron radiation flash. The detector noise in this time window was less than 0.03 Hz. The energy of the incident radiation was tuned by rotating the (10 6 4) channel-cut crystal in steps of 1.55 meV. The samples were mounted at a distance of $\approx$3 mm from the APD with an inclination angle of $\approx$10° relative to the incident beam providing good coverage of solid angle and illuminating a large sample volume.

We observed phonon spectra from metallic foils of α-iron and stainless steel $Fe_{0.55}Cr_{0.25}Ni_{0.2}$ with thicknesses of 10 and 30 μm, respectively. In addition, phonon spectra were taken from powder samples of strontium iron oxide, $SrFeO_x$ with $x = 2.5, 2.74, 2.86, 3.0$ and sample thicknesses of about 100 μm. The measurements were conducted at room temperature (298 K), and the samples were 95% enriched in ^{57}Fe. The collection time for each phonon spectrum ranged between 50 (stainless steel) and 100 min ($SrFeO_x$).

The main features of the observed phonon spectra are an elastic peak and sidebands at lower and higher energy (inset of Fig. 1). The elastic peak dominates the spectrum, as expected for solids with reasonable probability for recoilless absorption. Photons with less energy can excite the nuclear resonance by annihilation of a phonon (low energy sideband). The high energy sideband corresponds to phonon creation. Phonon annihilation is proportional to the temperature-dependent phonon occupation number, whereas the creation of phonons can also occur spontaneously, which explains the observed asymmetry in the spectra.

With the energy of the incident synchrotron radiation shifted by E relative to the nuclear resonance, the flux of delayed K-fluorescence photons emitted in the full solid angle is given by

$$I(E) = I_0 \rho \sigma \frac{\eta_K \alpha_K}{1 + \alpha} \frac{\pi}{2} \Gamma S(E), \qquad (1)$$

where I_0 is the incident photon flux, σ is the nuclear resonant cross section, η_K is the fluorescence yield, α, α_K are the total and partial internal conversion coefficients, respectively, and Γ is the nuclear level width. The effective area density of nuclei ρ also accounts for absorption within the material. $S(E)$ is the absorption probability per unit of energy. We will give it in terms of the quantum states $|\chi\rangle$ and the displacement operator $\hat{\mathbf{r}}$ of the nuclear motion

$$S(E) = \left\langle \frac{1}{dE} \sum_n |\langle \chi_n(E) | e^{-i\mathbf{k}\cdot\hat{\mathbf{r}}} | \chi_i \rangle|^2 \right\rangle_i . \qquad (2)$$

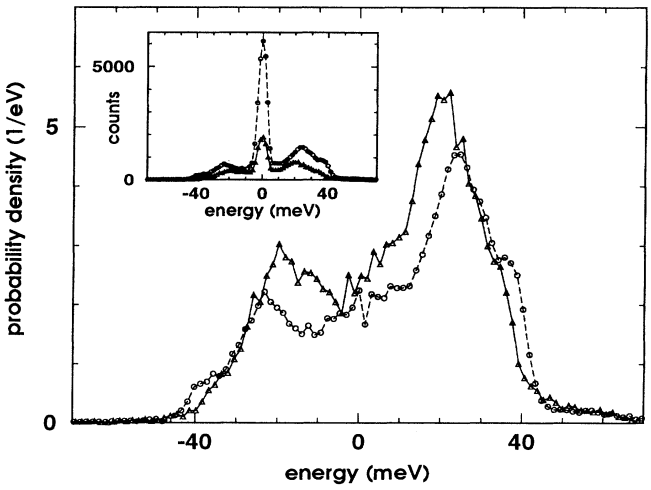

FIG. 1. The absorption probability density $S(E)$, as given in Eq. (2), is shown for α-iron (circles, dashed line) and stainless steel (triangles, solid line). The elastic peak is removed as described in the text. The inset shows the raw data.

The sum is over those intermediate states that differ by energies in the interval $[E, E + dE]$ from the initial state, and a thermal average is performed over the initial state. $\mathbf{k}$ is the wave vector of the incident radiation. $S(E)$ is normalized to unity. Its value in the wings of the phonon spectrum is estimated by $\overline{S} \approx (1 - f)/2k_BT$, where f is the recoilless fraction and k_BT is the thermal energy. In the present experiment, typical values were $f = 0.8$, $k_BT = 25$ meV, $\rho\sigma = 10^3$, $\Gamma\overline{S} = 2 \times 10^{-8}$, and $I_0 = 10^8$ Hz. The estimated flux of delayed fluorescence photons is then $\overline{I} = 10^3$ Hz. Further corrections for absorption in the sample, detector efficiency, and coverage of solid angle finally lead to the observed counting rates of ~20 Hz.

In extracting $S(E)$ from the measured data, one faces the problem of determining ρ for each sample. Difficulties occur because of the sharp increase in attenuation of the incident synchrotron radiation at the nuclear resonance. To illustrate the situation, we give the electronic and nuclear contributions to the attenuation length in the case of iron metal. The nuclear part is 0.09 μm at the elastic peak and takes an average value of 0.36 m in the wings of the spectra. The electronic part is constantly 20 μm. Therefore, for thick samples as in the present experiment, the effective number of nuclei that participate in the scattering is strongly decreased at the nuclear resonance and the elastic peak in the data is reduced in height by an essentially unknown factor. This normalization problem is solved by using the general property of $S(E)$ that its first moment equals the recoil energy $E_R = (\hbar^2k^2)/2M$ (1.94 meV for ^{57}Fe) of the nucleus [19]. This relation permits a calculation of the integrated inelastic spectrum A from the measured spectrum $I_m(E)$,

$$A = \frac{1}{E_R}\int I_m(E)E\,dE - \frac{1}{E_R}\int R(E)E\,dE\int I_m(E)\,dE\,. \tag{3}$$

The second term in this expression accounts for the slight correction that is necessary if the measured intensity $I_m(E)$, instead of $I(E)$ as given by Eq. (1), is used to calculate the first moment. The resolution function $R(E)$ gives the energy distribution of the incident synchrotron radiation and it is usually very close to being symmetric. Therefore, the correction term becomes very small. The phonon spectra are now easily normalized without complicated calculations of ρ that would involve sample geometry and composition. The pure phonon excitation spectrum results after the central peak is removed by fitting and subtraction. The normalized spectra of α-iron and stainless steel after removal of the central peak are shown in Fig. 1. The integrated spectra directly give the recoilless fraction or Lamb-Mössbauer factor

$$f = 1 - \frac{1}{A}\int I'_m(E)\,dE\,, \tag{4}$$

where $I'_m(E)$ denotes the phonon spectrum after removal of the central peak. In contrast to Mössbauer transmission spectroscopy [20] and synchrotron radiation Mössbauer spectroscopy [11,21], Eq. (4) does not require specific knowledge about isotopic abundance, shape or thickness of the sample, resonant cross section, or hyperfine interactions. The Lamb-Mössbauer factor of α-iron was determined to be $f = 0.805(3)$. From the phonon DOS, as shown in Fig. 2, we calculated the recoilless fraction at zero temperature to be $f_0 = 0.9241(7)$ and a ratio of $f/f_0 = 0.871(4)$. This is in agreement with earlier results of $f/f_0 = 0.866(3)$ [11].

For further processing of the data, we assumed the sample material to behave like a harmonic lattice with well-defined phonon states. An expansion of $S(E)$ in terms of n phonon contributions is then straightforward [22]

$$\begin{aligned} S(E) &= f\delta(0) + f\sum_{n=1}^{\infty} S_n(E)\,, \\ S_1(E) &= \frac{E_R\mathcal{D}(E)}{E(1 - e^{-\beta E})}\,, \\ S_n(E) &= \frac{1}{n}\int S_{n-1}(E - \epsilon)S_1(\epsilon)\,d\epsilon, \qquad n \geq 2\,. \end{aligned} \tag{5}$$

The phonon DOS $\mathcal{D}(E)$ is proportional to the one-phonon term in this expansion. Generally the ratio of the n- and $(n - 1)$-phonon terms is given by $-(\ln f)/n$, which results in a multiphonon contribution of less than 15% for the present data. We deconvoluted the measured

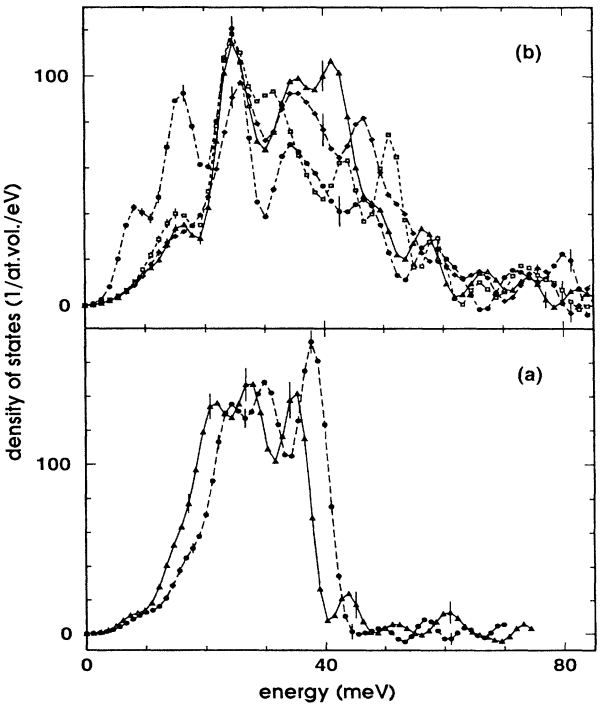

FIG. 2. The phonon DOS of different materials are shown. (a) α-iron (circles, dashed line) and stainless steel (triangles, solid line). (b) $SrFeO_x$ with $x = 3$ (triangles, solid line), $x = 2.86$ (diamonds, dashed line), $x = 2.74$ (rectangles, dotted line), and $x = 2.5$ (circles, dashed-dotted line).

spectra with the resolution function that was fitted to the central peak and applied Eq. (5) to recover the phonon DOS. The results are shown in Fig. 2. In the case of α-iron, $\mathcal{D}(E)$ shows several critical points as predicted [2], although the features are smeared out, most likely due to phonon lifetime effects. The structures above 45 meV are residuals that arise from the deconvolution procedure. If the energy scale of the phonon DOS of stainless steel is stretched by 8%, then the acoustic modes exhibit strong similarities with those of α-iron. This indicates a reduced coupling of about 16%, which might be related to the change in local symmetry from bcc for α-iron to fcc for stainless steel. Dramatic differences occur in the phonon DOS of $SrFeO_x$ while the system undergoes structural changes from cubic perovskite for $x = 3.0$ to tetragonal perovskite with vacancy ordering for $x = 2.86$ to orthohombic perovskite with vacancy ordering for $x = 2.74$ and finally to brownmillerritelike orthorhombic for $x = 2.5$ [23]. Most striking are the persistent phonon modes at 25 meV and the increase of soft-phonon modes at 8 and 16 meV for the brownmilleritelike structure.

From the phonon DOS, we derived the vibrational contribution to the specific heat at constant volume. For α-iron, we determine a value of 23.8(3) J/K mol. The difference between this value and the thermometrically determined value 25.1 J/K mol [24] is attributed to the electronic contribution to the specific heat. It was measured as 1.5 J/K mol [25], which is in agreement with the present evaluation.

In conclusion, we presented measurements of phonon DOS by inelastic nuclear resonant scattering of synchrotron radiation for a number of compounds. This technique allows direct determination of phonon DOS for small samples ($\approx$3 mg in the present experiment) with excellent signal-to-noise ratio ($S/N \approx 10^3$) in a very short time (several minutes at third-generation synchrotron radiation sources). The energy resolution is variable and can be reduced to $\sim$1 meV using crystal optics or even to μeV levels via nuclear resonant filtering of the incident synchrotron radiation. The information that can be derived from such measurements can be used to support existing or develop new models for the interatomic forces and for the coupling of phonons to other quasiparticles. Thus, for example, vibrational entropies and other thermodynamical properties of order-disorder alloys can be studied and temperature-dependent phonon spectra can provide data about the phonon interaction. In addition, materials with noncrystalline structure, such as glasses and liquids, can easily be investigated on the basis of a trend analysis.

The authors acknowledge the support of the TRISTAN accelerator group at KEK. The work at Argonne is supported by the U.S. Department of Energy BES-Materials Science under Contract No. W-31-109-ENG-38. The work at NIU is supported by NSE (Contract No. DMR 93-10656) and the State of Illinois under HECA.

[1] B.N. Brockhouse, in *Inelastic Scattering of Neutrons in Solids and Liquids* (International Atomic Energy Agency, Vienna, 1961).
[2] V.J. Minkievicz, G. Shirane, and R. Nathans, Phys. Rev. **162**, 528 (1967).
[3] B.N. Brockhouse, H. Abou-Helal, and E.D.. Hallmann, Solid State Commun. **5**, 211 (1967).
[4] G. Gilat and L.J. Raubenheimer, Phys. Rev. **144**, 390 (1965).
[5] E. Burkel, *Inelastic Scattering of x-Rays with Very High Energy Resolution* (Springer-Verlag, New York, 1991).
[6] M. Seto, Y. Yoda, S. Kikuta, X.W. Zhang, and M. Ando, preceding Letter, Phys. Rev. Lett. **74**, xxxx (1995).
[7] E. Gerdau, R. Rüffer, H. Winkler, W. Tolksdorf, C.P. Klages, and J.P. Hannon, Phys. Rev. Lett. **54**, 835 (1985).
[8] W. Sturhahn, E. Gerdau, R. Hollatz, R. Rüffer, H.D. Rüter, and W. Tolksdorf, Europhys. Lett. **14**, 821 (1991).
[9] E.E. Alp, T.M. Mooney, T.S. Toellner, W. Sturhahn, E. Witthoff, R. Röhlsberger, E. Gerdau, H. Homma, and M. Kentjana, Phys. Rev. Lett. **70**, 3351 (1993).
[10] W. Sturhahn and E. Gerdau, Phys. Rev. B **49**, 9285 (1994).
[11] U. Bergmann, S.D. Shastri, D.P. Siddons, B.W. Batterman, and J.B. Hastings, Phys. Rev. B **50**, 5957 (1994).
[12] R.L. Cohen, G.L. Miller, and K.W. West, Phys. Rev. Lett. **41**, 381 (1978).
[13] U. Bergmann, J.B. Hastings, and D.P. Siddons, Phys. Rev. B **49**, 1513 (1994).
[14] L. Van Hove, Phys. Rev. **95**, 249 (1954).
[15] K.S. Singwi and A. Sjölander, Phys. Rev. **120**, 1093 (1960).
[16] X. Zhang, T. Mochizuki, H. Sugiyama, S. Yamamoto, H. Kitamura, T. Sioya, M. Ando, Y. Yoda, T. Ishikawa, S. Kikuta, and C.K. Suzuki, Rev. Sci. Instrum. **63**, 404 (1992).
[17] T.M. Mooney, T.S. Toellner, W. Sturhahn, E.E. Alp, and S.D. Shastri, Nucl. Instrum. Methods Phys. Res., Sect. A **347**, 348 (1994).
[18] T.S. Toellner, W. Sturhahn, E.E. Alp, P.A. Montano, and M. Ramanathan, Nucl. Instrum. Methods Phys. Res., Sect. A **350**, 595 (1994).
[19] H.J. Lipkin, Ann. Phys. (Paris) **9**, 332 (1960).
[20] B.R. Bullard, J.G. Mullen, and G. Schupp, Phys. Rev. B **43**, 7405 (1991).
[21] E.E. Alp, W. Sturhahn, and T.S. Toellner, Nucl. Instrum. Mehods Phys. Res., Sect. B (to be published).
[22] W. Marshall and S.W. Lovesey, *Theory of Thermal Neutron Scattering* (Oxford University Press, London, 1971).
[23] Y. Takeda, K. Kanno, T. Takada, O. Yamamoto, M. Takano, N. Nakayama, and Y. Bando, J. Solid State Chem. **63**, 237 (1986).
[24] L.S. Darken and R.P. Smith, Ind. Eng. Chem. **43**, 1815 (1951).
[25] N.W. Ashcroft and N.D. Mermin, *Solid State Physics* (W.B. Saunders Company, Philadelphia, 1976).